OLUME 58 / NUMBER 8 / NOVEMBER 21, 1995

Journal of

APPLIED POLYMER SCIENCE

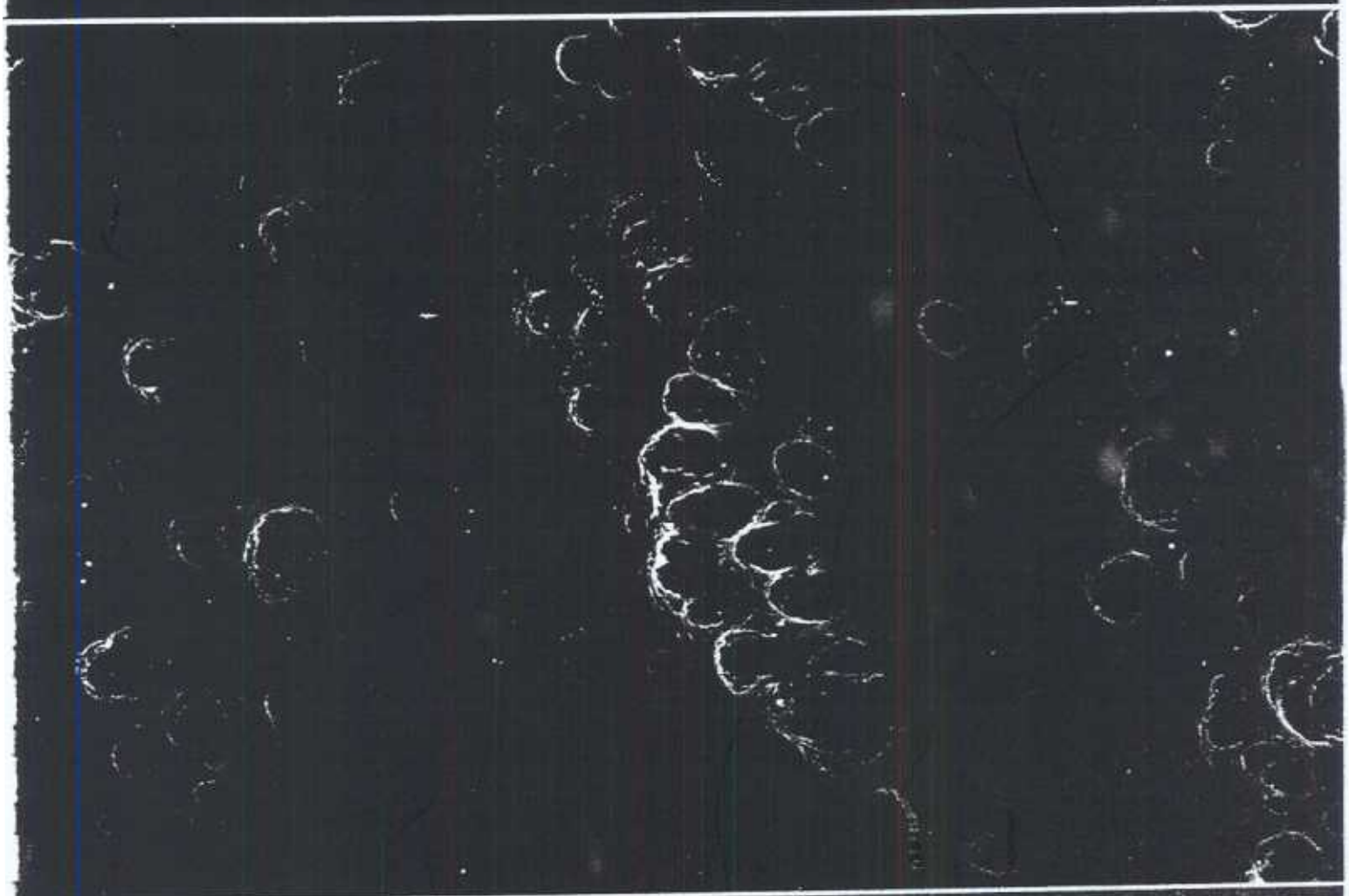

WILEY
Publishers Since 1807
New York • Chichester • Brisbane • Toronto • Singapore

Journal of
APPLIED POLYMER SCIENCE

VOLUME 58 / NUMBER 8 / NOVEMBER 21, 1995

CONTENTS

(Continued)

Preparation and Characterization of Cellulose Acetate Organic/Inorganic Hybrid Films

SAEED S. SHOJAIE,[1] TIMOTHY G. RIALS,[2,*] and STEPHEN S. KELLEY[1]

[1]National Renewable Energy Laboratory, 1617 Cole Blvd., Golden, Colorado 80401; [2]Southern Forestry Experiment Station, 2500 Shreveport Hwy., Pineville, Louisiana 71360

SYNOPSIS

A series of organic/inorganic hybrid (OIH) films were prepared using cellulose acetate (CA) as the organic component and tetraethyl orthosilicate (TEOS) as the inorganic component. The chemical, morphological, and mechanical properties of these films were evaluated with a variety of analytical techniques. The results of these evaluations showed that crosslinked CA OIH films were formed during the sol-gel reactions. The structure of OIH films was very sensitive to the CA/TEOS ratio and film formation conditions. All of the films with added TEOS were two phase on a molecular level, i.e., inorganic TEOS domains surrounded by a CA matrix. Under some film formation conditions the presence of TEOS, a nonsolvent for CA, led to solvent/nonsolvent phase separation on the micron scale. © 1995 John Wiley & Sons, Inc.

INTRODUCTION

Sol-gel chemistry was introduced over 30 years ago.[1,2] This process was originally developed as an alternative method for manufacturing ultrahigh purity glasses. The traditional sol-gel is a chemical process by which glassy materials can be formed from a homogeneous solution through a series of hydrolysis and condensation reactions with a variety of metal alkoxides. A highly schematic example of the reaction sequence is shown below:

$$M(OR)_n + nH_2O \rightarrow M(OH)_n + nROH$$

$$M(OH)_n \rightarrow MO_{n/2} + (n/2)H_2O$$

where M is a metal such as Si, Al, Ti, or other transition element, and R is an alkyl group such as methyl, ethyl, etc. The hydrolysis and polycondensation reactions are catalyzed by acids or bases. The nature of catalyst also influences the final material morphology.[3,4]

The sol-gel process has a number of advantages over traditional high temperature fusion techniques.[5,6] The homogeneous starting solutions used in the sol-gel process allow for production of glasses with higher purity and homogeneity than those formed with traditional techniques. It also offers the potential for forming mixed metal oxide glasses that cannot be easily formed with the standard heat fusion process owing to limitations of crystallization and phase separation phenomena. Because the initial reaction sequence is conducted at low temperature, there is potential for substantial energy savings. However, owing to the considerable shrinkage that can occur during the curing step, it is difficult to obtain large defect-free monoliths.

In recent years, the sol-gel process has been used for the preparation of novel organic/inorganic hybrid (OIH) materials. OIH materials are generated from a homogeneous starting solution consisting of a reactive organic component, oligomer or polymer, and a metal alkoxide inorganic component. This mixture is polymerized into a gel using the hydrolysis and condensation reactions that are typical of the traditional sol-gel process. The gelled matrix may be processed into a solid matrix via postformation curing step. By varying the chemical composition of the organic and inorganic oligomeric and polymeric components, the rates of the competing hydrolysis and condensa-

* To whom correspondence should be addressed.

Journal of Applied Polymer Science, Vol. 58, 1263–1274 (1995)
 CCC 0021-8995/95/081263-12

tion reactions, and the physical conditions in which the OIH material is produced, one can obtain OIH materials with a wide range of chemical, mechanical, and thermal properties.

OIH materials can be used to increase the mechanical and thermal properties of rubbery polymers. The crosslinking reactions that occur during formation of OIH materials can increase the chemical stability or resistance to swelling of the organic component. Molecular level porosity can be introduced into OIH materials through the use of difunctional inorganics that are coupled with a labile organic spacer. In addition to influencing chemical, mechanical, or thermal properties, OIH materials can be used for the preparation of unique composites. The OIH process has been used for the preparation of novel filters, displays, or optical storage devices if the organic component has its own unique characteristics, e.g., nonlinear optical or photochromic properties. During the last decade, a number of researchers have focused on synthesizing OIH materials for applications such as hard contact lenses,[7] defect-free monoliths,[8] sensors, and displays, as well as, the formation of glass with improved mechanical properties.

Cellulose acetate (CA) is a thermoplastic polymer produced primarily from cellulose, a renewable feedstock. CA has applications in many areas such as supports for fibers, plastics, photographic film, and coatings for pharmaceuticals. These advantageous properties are balanced out by several limitations including poor resistance to mechanical creep, and limited resistance to organic solvents. Preparation of CA-based OIH materials is one potential route for overcoming these limitations. The objectives of this work are: (1) to prepare a functionalized cellulose acetate polymer that can be used as the organic component in OIH materials prepared through the sol–gel process; (2) to characterize the physical properties of the resulting OIH materials; and (3) to elucidate the role of important sol–gel formation parameters on the final morphology and physical properties of the OIH materials.

EXPERIMENTAL

Materials

Cellulose acetate (CA-398-30) with an acetyl degree of substitution [the degree of substitution (DS) is a measure of the number of cellulose hydroxyls that have been reacted] of 2.45 and a number average molecular weight of 60,000 was obtained from Eastman Chemical Company and used as the organic component in this study. Tetraethyl orthosilicate (TEOS) of 98% purity was obtained from Aldrich and used as the inorganic component. The 3-isocyanatopropyl triethoxysilane and dibutyltin dilaurate were obtained from Lancaster. All other chemicals used in this study were of reagent grade and were used as received.

Functionalization of Cellulose Acetate

CA was chemically modified at two different levels of functional groups. These samples were prepared through the reaction of 3-isocyanatopropyl triethoxysilane with the free hydroxyl[9] on the CA backbone. The grafting level of triethoxysilane is controlled by the initial mol ratio of polymer to 3-isocyanatopropyl triethoxysilane. The two grafted polymer samples prepared for this study have approximately one grafted substituent per 10 CA repeat units (CAG^+) and one grafted substituent per 27 CA repeat units (CAG^-). The procedure for preparing CAG^+ is given below as an example. A homogeneous solution of 60.42 g (0.226 mol assuming a monomeric molecular weight of 267) CA-398-30 in 570 g tetrahydrofuran was prepared by vigorously mixing the solution under a nitrogen blanket. To this mixture 5.36 g (0.022 mol) of 3-isocyanatopropyl triethoxysilane and 0.41 g (0.0006 mol) of dibutyltin dilaurate catalyst were added. The mixture was heated to 60°C and mixed rapidly for 6 h under a blanket of nitrogen. The progress of the reaction was monitored by taking infrared spectra of the polymer solution at various reaction times. When the reaction was complete (as measured by FTIR), the mixture then was precipitated in anhydrous ether. The resulting polymer was dried under vacuum for 24 h, stored under nitrogen, and used for the subsequent preparation of OIH films.

OIH Film Formation

The grafted CA polymers (CAG^+, CAG^-) and unmodified CA were used as the organic component of OIH films cast from solution. A description of the procedure used for casting film #7 of Table I is given below as an example of the casting technique. A homogenous solution of 4.01 g of CAG^+ in 32.53 acetone was prepared. The solution then was filtered through a 7 μm filter element. TEOS (4.06 g) was

Table I Composition and Properties of the Cast Films

Film Number	Polymer	Wt % TEOS	TEOS/HCl Mol Ratio	H_2O/TEOS Mol Ratio	Acetone Solubility	Phase Separation
1	CA	0	—	—	Y	N
2	CAG^+	0	—	—	Y	N
3	CAG^+	30	30	4	N	N
4	CAG^-	30	31	9	N	N
5	CAG^+	30	57	10	N	Y
6	CAG^-	30	79	4	N	N
7	CAG^+	50	77	4	N	N
8	CAG^-	50	70	2	N	N
9	CAG^+	50	132	2	N	Y
10	CAG^-	50	144	4	N	N

added to the CAG^+ solution, causing the formation of a small amount of a white precipitate. The precipitate was easily redissolved with additional stirring of the CAG^+/TEOS solution. A mixture of 1.38 g deionized water and 0.01 g of hydrochloric acid was added to the CAG^+/TEOS/acetone solution and mixed vigorously. The mixture was allowed to react for approximately 8 min. The solution was degassed and cast on Teflon tape mounted on a 30 × 30 cm glass plate with a casting knife at an initial film thickness of 1000 μm. The film was kept under a saturated acetone environment for approximately 2 h. After the complete evaporation of acetone, the film was removed from the Teflon tape and was placed under vacuum at 50°C for 24 h. The final dimensions of the cast film were 14 × 23 cm × 0.05 to 0.18 mm thick. All the films cast in this manner were then used in the subsequent analyses without any further treatment.

Analysis Techniques

Infrared spectra were obtained using a Nicolet 5SXC FT-IR spectrometer. Thermal analyses were conducted on a TA Instruments 2950 thermogravimetric analyzer (TGA). Gravimetric measurements were made over the 40–750°C range with a 20°C/min scan rate under a constant air flow. Solid-state ^{29}Si cross polarization magic angle spinning (CP/MAS) nuclear magnetic resonance (NMR) spectra were acquired using a modified Nicolet NT-200 NMR spectrometer using a 1 ms contact time and a 1 s recycle delay. The equilibrium mass loss data were obtained by measuring the dry weight of the specimens before and after a 48-h immersion in acetone. Dynamic mechanical analysis (DMA) data were obtained using a Rheometrics RSA-2. Stress-strain measurements were obtained using films of 70 mm long, 10 mm wide, and 0.05 to 0.18 mm thick on an Instron model 1122. The properties of four or five films were averaged to obtain values for the mechanical properties. Structural details were obtain using a Cambridge 250MK3 scanning electron microscope (SEM).

RESULTS

Chemical Modification of Cellulose Acetate

CA was chemically modified by the addition of triethoxysilane groups to promote crosslinking among polymer molecules. The chemical structure of the CAG backbone is schematically shown below:

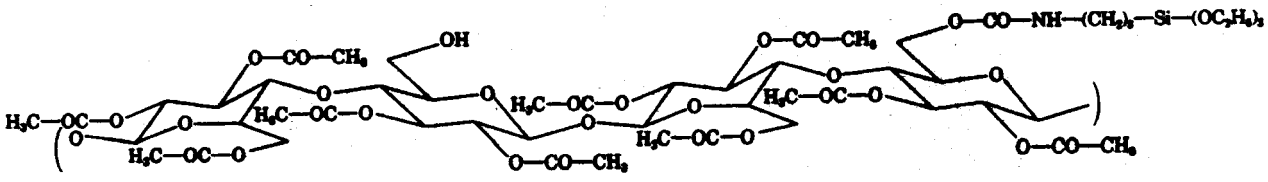

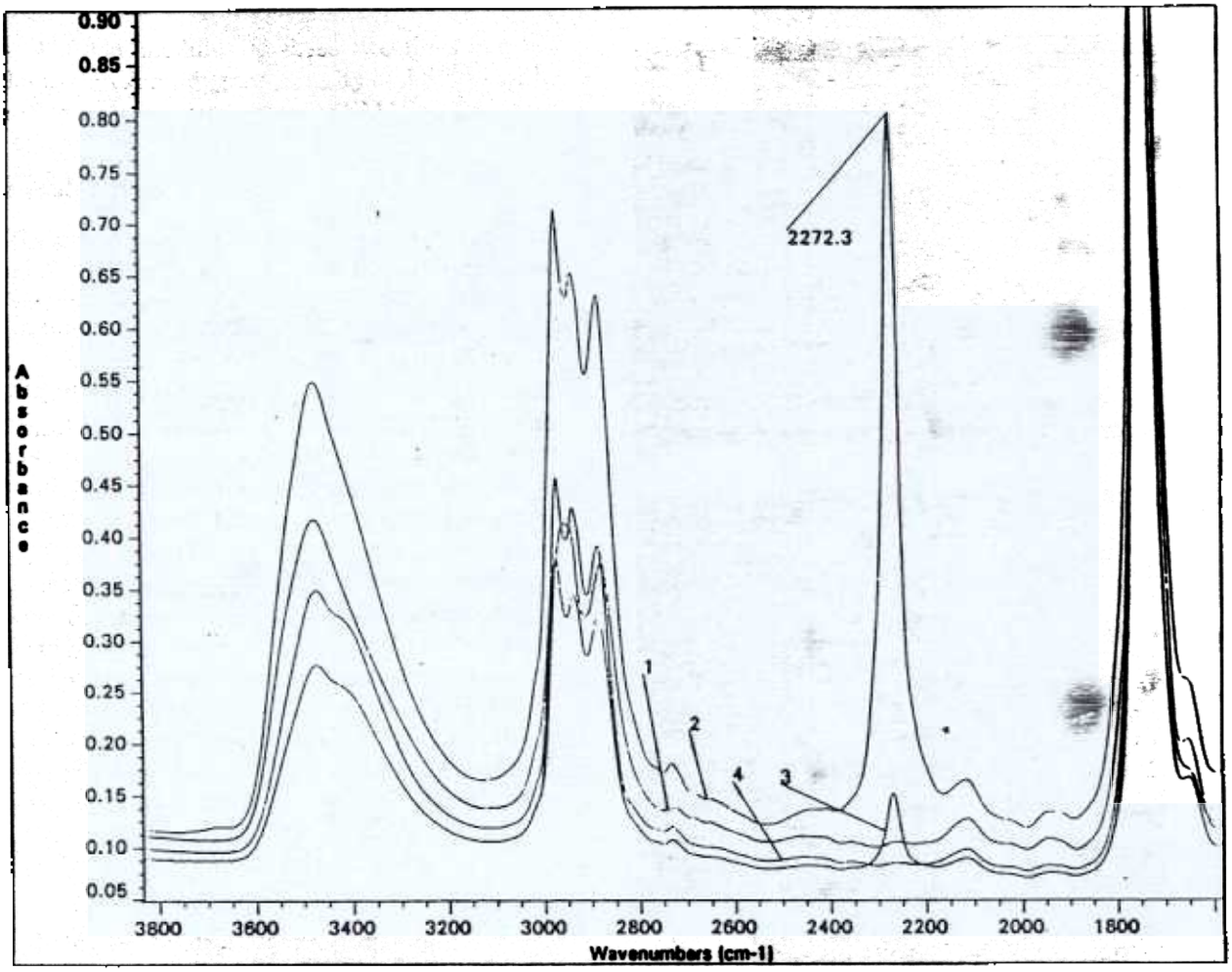

Figure 1 Fourier transform infrared (FTIR) spectra of polymer solution during reaction of free hydroxyls on the polymer with 3-isocyanatopropyl triethoxysilane showing the disappearance of isocyanate linkage.

It is important to note that the CAG contains residual, unreacted hydroxyls on the polymer backbone. These residual hydroxyls are available for condensation reactions with silanol groups on either the triethoxysilane groups grafted onto CA or TEOS. The direct reaction of the free hydroxyls with silane groups could create additional sites for crosslinking the CA chains.

During the grafting reaction, the disappearance of the N=C=O group of the isocyanate was monitored with the infrared spectroscopy. Figure 1 shows FTIR spectra of thin films cast from the CA/3-isocyanatopropyl triethoxysilane reaction mixture as a function of reaction time. Spectra are labeled 1 to 4, corresponding to reaction times of 0, 0.17, 2, and 5.5 h, respectively. A reaction time of zero corresponds to polymer solution prior to the addition of 3-isocyanatopropyl triethoxysilane and dibutyltin dilaurate. Spectrum 1 does not show a strong absorbance at 2272.3 cm^{-1}, while spectrum 2, taken shortly after the addition of the 3-isocyanatopropyl triethoxysilane, shows a large increase in absorbance at the same wave number characteristic of the N=C=O group. The intensity of this peak diminishes with increasing reaction time until 5.5 h after the start of the reaction where the spectra 4 and 1 are very similar in the region of 2200 to 2300 cm^{-1}, indicating the complete disappearance of isocyanate group. The reaction mixture was immediately quenched because prior experience indicated that prolonged reaction times could lead to gelation of the solution. This gelation was not investigated but is presumably because of reactions among the grafted triethoxysilane groups

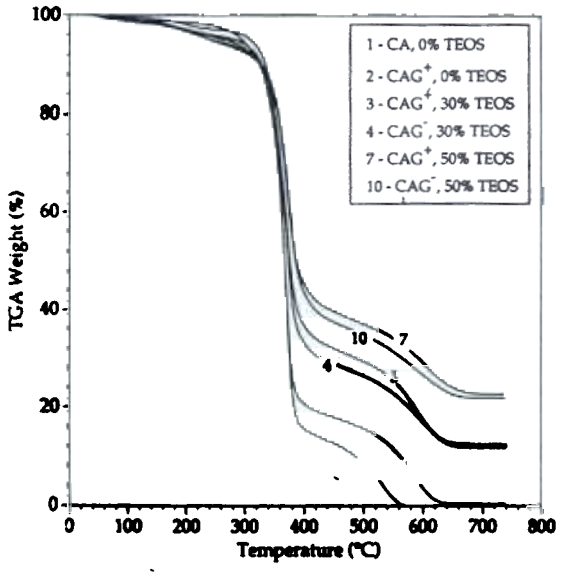

Figure 2 Thermogravimetric data showing the decomposition behavior of OIH films. Curve numbers correspond to the film numbers in Table I.

and between triethoxysilane and free hydroxyls on the CA.

Composition of Cast Films

Table I shows the composition of the solutions used in this study for preparation of films. The film number, polymer type, weight percent TEOS based on CA polymer weight, and TEOS/HCl and H_2O/TEOS mol ratios are given in the first five columns of Table I, respectively. The organic component of these OIH films was unmodified CA and grafted CA containing two levels of crosslinkable pendant triethoxysilane groups. Films 1 and 2 were cast from CA and CAG^+ without any added TEOS, water, or catalyst, and should be homogeneous at the molecular level. Films 4, 6, 8, and 10 were cast using CAG^- polymer at various levels of reactants and should be less highly crosslinked than films 3, 5, 7, and 9, which were cast from solutions of CAG^+.

Thermogravimetric Experiments

Thermogravimetric experiments were used to determine the inorganic content of these composite materials. Thermogravimetric measurements of percent weight loss vs. temperature are shown in Figure 2. The numbers associated with the curves correspond to the film numbers of Table I. The CA specimen (curve 1) underwent complete decomposition; that is, the final weight is zero. The CAG^+ specimen with 0% TEOS (curve 2) displays a very similar weight-temperature behavior. Films 3 and 4, which were cast from CAG^+ and CAG^- polymers, respectively, with 30% TEOS have approximately the same residual weight at 750°C. The corresponding films with 50% initial TEOS (curves 7 and 10) also show a similar thermogravimetric behavior. As expected, the residual weights progressively increase as the initial TEOS concentration increases, e.g., curves 2, 3, and 7. The theoretical calculation of residual weights based on 100% conversion of TEOS into SiO_2 were in close agreement with the experimental values.

The presence of additional crosslinks appears to affect the weight loss profile at temperatures between 400°C and 600°C. In each case, the CAG^+-based OIH films show less weight loss in this temperature range than the CAG^--based OIH films. This difference may be due to restricted molecular mobility in the case of the CAG^+-based OIH films that allows for the formation of greater amounts of char.

Chemical Structure of the Inorganic Component

A representative ^{29}Si CP/MAS spectrum of OIH film is shown in Figure 3. The peaks can be assigned based on the results from previous studies of TEOS-based multifunctional sol–gel materials.[10] The group of peaks between −40 and −65 ppm can be assigned to silicon bonded to three oxygens and 1 carbon (T-type silicon) and arise from the silicons in the CA-grafted triethoxy sidechains. The peaks at ∼−45, ∼−56, and ∼−63 ppm can be assigned to silicons in T^1 (two unreacted ethoxy groups), T^2 (one unreacted ethoxy groups), and T^3 (no unreacted ethoxy groups) type structures, respectively. The group of peaks between −80 and −110 ppm can be assigned to silicon bonded to four oxygens (Q-type silicon) arising from silicons in the siloxane polymer formed as a result of the TEOS condensation reactions. The peaks at ∼−80, ∼−88, ∼−96, and ∼−106 ppm can be assigned to Q^1 (three unreacted R groups), Q^2 (two unreacted R groups), Q^3 (one unreacted R groups), and Q^4 (no unreacted R groups), respectively.

The presence of both T^2 and T^3-type silicon demonstrates the formation of direct crosslinks between the CA-grafted triethoxy substituents and other CA-grafted triethoxy substituents and/or TEOS. The presence of the Q^3 and Q^4 peaks demonstrate the formation of branched and fully reacted structures within the TEOS component. Formation

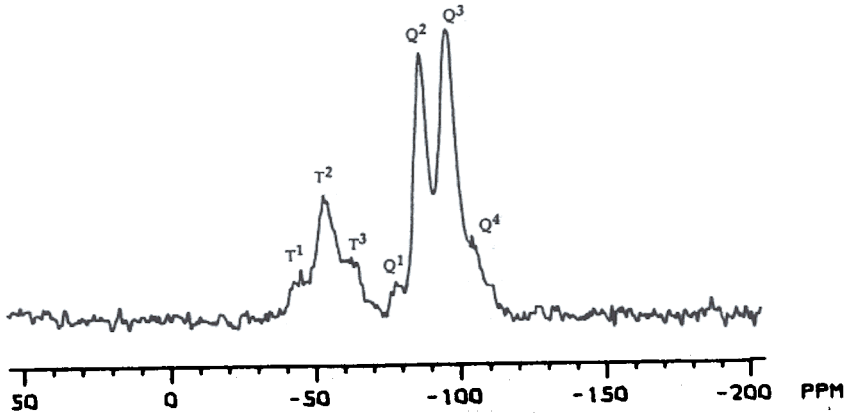

Figure 3 Solid-state NMR (^{29}Si) of a representative OIH film.

of these types of structures should lead crosslinking of the CA organic component within the OIH material. However, the presence of the T^1, Q^1, and Q^2 structures indicates that the condensation reactions were incomplete for both the grafted triethoxysilane and the TEOS.

Solubility Properties

The acetone solubility of the cast films is shown in column 6 of Table I. All the films except 1 and 2 remained insoluble in acetone after 48 h of immersion. As expected, films 1 and 2, which were prepared without the addition of TEOS or acid catalyst, dissolved in acetone. Figure 4 shows percent inorganic-free mass loss as a function of TEOS/HCl mol ratio for films cast from CAG^-. These data represent the percent mass loss after the films have been immersed in an acetone bath for 48 h. (No mass loss data for specimens 1 and 2 are shown because these specimens dissolved in acetone. Accurate mass loss measurements for films 5 and 9 could not be obtained because both films had phase spearated. As a result, no mass loss data for the CAG^+ series is reported.)

The solvent resistance of these OIH films is very sensitive to the number of polymer–polymer and polymer–TEOS–polymer crosslinks. Dissolution of films 1 and 2 is consistent with a polymer matrix devoid of any crosslinks. For the remainder of the films, there are two competing effects that control the number of crosslinking junctions within the OIH film: the effects of chemical crosslinking, and the evaporation of casting solvent. The first effect is relative to the rate of the hydrolysis and condensation reactions that occur within the inorganic component. For a completely closed system (i.e., absence of solvent evaporation), the faster the rate of reaction, the shorter the gel time. The second effect is related to physical gelation of the OIH solution caused by solvent loss from the casting solution. Solvent evaporation causes an increase in viscosity, physical gelation, and, finally, solidification of the OIH system. This physical gelation reduces the mobility of the reactive sites on the polymer chains limiting the formation of crosslinking of polymer chains.

Increasing the TEOS/HCl mol ratio reduces the number of crosslinks that can form prior to gelation caused by solvent evaporation. This effect, in turn, can result in a delay in the onset of gelation time, which can cause an increase in the number of cross-

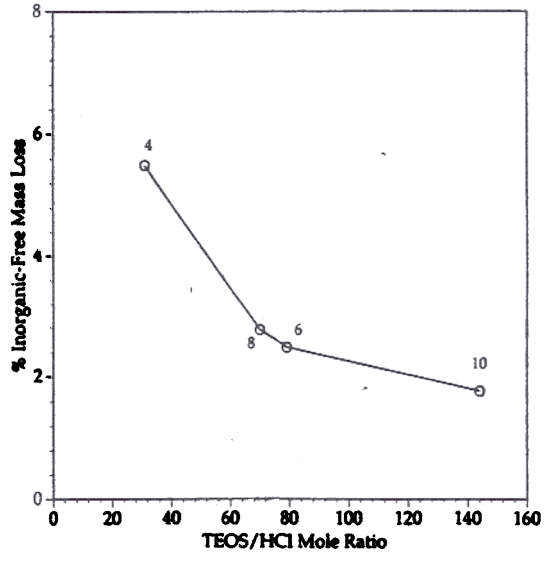

Figure 4 Inorganic-free mass loss of films cast from CAG^- as a function of TEOS/HCl mol ratio in the initial casting solution. Numbers correspond to the film numbers of Table I.

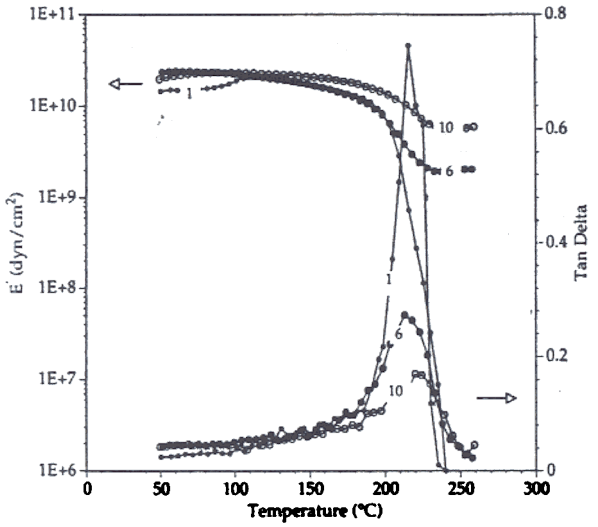

Figure 5 Storage (left ordinate) and loss (right ordinate) moduli as a function of temperature for films 1, 6, and 10 of Table I.

links, assuming the effect of acetone evaporation remains constant. The net effect is to increase the overall number of crosslinks in the polymer matrix and, hence, decrease the number of free polymer molecules. Therefore, one would expect to observe a decreasing trend in the mass loss (dissolution of free polymer molecules in acetone) with increasing TEOS/HCl mol ratio. The decreasing trend in mass loss is clearly observed with CAG^- films in Figure 4. The same argument should hold true for the CAG^+ films. However, one can expect a further reduction in the mass loss because of a higher number of available crosslinkable sites.

Dynamic Mechanical Analyses

Dynamic mechanical analysis (DMA) was used to evaluate the network structure of the CA OIH films. The effect of TEOS concentration in the initial polymer solution on the dynamic mechanical behavior is shown in Figure 5. Storage modulus, E′, (left ordinate) and loss tangent (tan δ) (right ordinate) data as a function of temperature for films 1 (0% TEOS), 6 (30% TEOS), and 10 (50% TEOS) are presented in this figure. All of the films have very similar behavior in the glassy region (50–200°C), within the measurement accuracy. These films also show a broad glass transition (T_g) region (190–240°C). The unmodified CA (film 1) begins to undergo viscoelastic flow as evidenced by the sharp drop in the log E′ at approximately 240°C. In contrast, films 6 and 10, which were cast from CAG^- solutions with 30 and 50% TEOS, respectively, show a rubbery plateau region (> 240°C). This behavior is indicative of a crosslinked material above its T_g. The magnitude of the storage modulus in the rubbery plateau region increases with increasing TEOS concentration. An increase in the modulus of the rubbery plateau with increasing TEOS content may be because of a higher crosslink density of the network or a higher inorganic filler content. The mass loss experiments (Fig. 4) indicate that the higher TEOS content does lead to a higher crosslink density. Crosslinking may also effect the T_g of the organic component of the OIH material. There is a slight increase in T_g as delineated by the maximum of the tan δ response with an increase in the initial TEOS concentration.

Figure 6 shows the dynamic mechanical behavior of films 7 and 10, which were cast from CAG^+ and CAG^-, respectively, with 50% initial TEOS. Both of these OIH materials behave like crosslinked networks. However, within the reproducibility of these experiments, there are no significant differences in the magnitude of the storage modulus of the rubbery plateau. The behavior of these films indicates that the level of grafting does not have a significant influence on the mechanical properties of these OIH materials above their T_g. One also can speculate that the effect of the grafting level becomes less pronounced at this high level of TEOS (50%) owing to the increased crosslinking condensation of free hydroxyl on the CA backbone through the TEOS network.

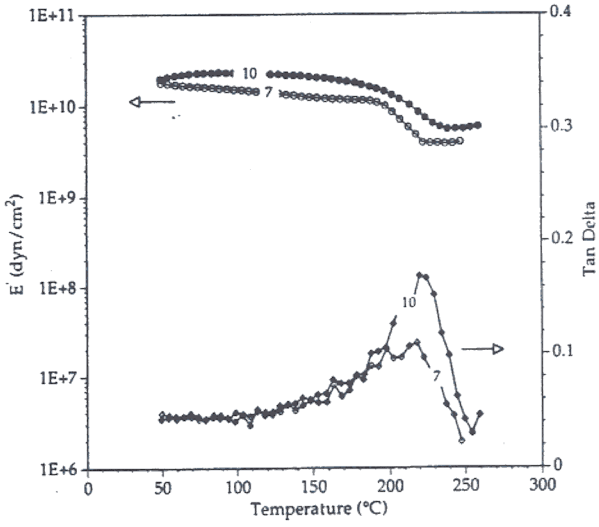

Figure 6 Storage (left ordinate) and loss (right ordinate) moduli as a function of temperature for films 7 and 10 of Table I

Stress–Strain Measurements

Representative stress–strain behavior of hybrid materials is shown in Figure 7. The mechanical behavior for films 2 and 8 of Table I are given by the symbols (□) and (■), respectively. (The data presented in Fig. 7 were obtained from four to five separate tests on each OIH film.) The dashed and solid lines are spline curve fit of the experimental data. Both films exhibit stress–strain response typical of tough plastic materials, i.e., an initial rapid increase in the stress followed by an elongation period where the stress remains relatively constant with increasing strain. It is apparent that the addition of 50% TEOS (film 8) increases the tensile strength significantly while it decreases the elongation. This may be attributed to the presence of brittle SiO_2 phase.

The average elastic modulus as a function of TEOS/HCl mol ratio for all the films in Table I is shown in Figure 8. The numbers associated with the data correspond to the film numbers in Table I. The error bars for the CAG^- are not shown; however, they are very similar in magnitude to CAG^+ series. It is apparent that there is no significant difference between the modulus of films 1 and 2. These results indicate the presence of unreacted, grafted groups does not have a significant influence on the modulus of the film.

The films cast from CAG^- (●) show a slight increase in modulus with increasing TEOS/HCl ratio, while films cast from CAG^+ (○) do not exhibit any

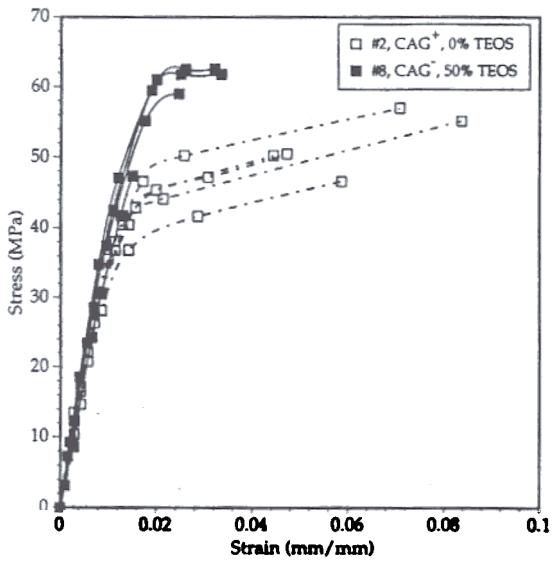

Figure 7 Stress–strain measurements corresponding to films 2 (□) and 8 (■) of Table I.

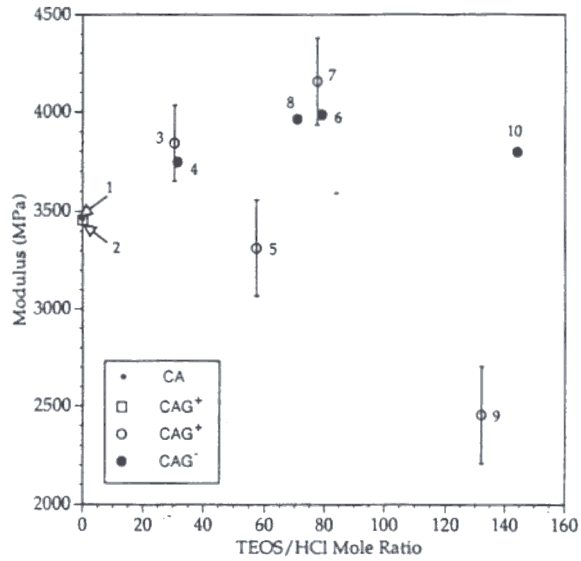

Figure 8 Modulus of all the films of Table I as a function of TEOS/HCl mol ratio.

trend with increasing TEOS/HCl ratio. Changes in mechanical properties with the formation of crosslinking sites and the addition of an inorganic filler are expected for these OIH materials. A slight increase in moduli of films cast from CAG^- (large filled circle) over those of CA (small filled circle) and CAG^+ (large open square) (not crosslinked) is observed as shown in Figure 8. However, the elastic modulus of CAG^- films appears to be insensitive to the composition of the OIH films (films 4, 6, 8, and 10). The small change in the modulus of OIH films over that of the CA film can be attributed to the fact that all of these OIH materials were prepared from a glassy polymer with a relatively high modulus. Thus, the presence of crosslinking sites and the addition of an inorganic filler associated with the formation of the OIH films does not have a significant impact on the modulus of the OIH films in the glassy state. In contrast, the DMA results indicated that the presence of crosslink sites does have a substantial influence over modulus of the OIH films in the rubbery state.

The effect of the number of crosslinking sites can be evaluated by comparing the OIH films prepared from CAG^- to those prepared from CAG^+. Films 3 and 7, which were prepared from CAG^+, show similar stress–strain behavior to those prepared from CAG^- films (films 4, 6, and 8). Within the experimental error, the moduli of these OIH films are essentially the same whether they were prepared from CAG^+ or CAG^- starting materials. However, films 5 and 9 show a significant reduction in their mod-

ulus. The low modulus of these two films can be explained by examining the porosity of the films with scanning electron microscopy (SEM).

SEM Examination

All the cast films were transparent except those of 5 and 9, which were opaque, as indicated in column 7 of Table I. Representative cross-sectional views of OIH films are shown in Figure 9. Figures 9(a), (b), and (c) correspond to the films 3, 5, and 9 of Table I, respectively. Features in Figure 9(a) do not reveal any signs of macrophase separation with 30% initial TEOS concentration. This observation is consistent with the fact that this film is transparent, indicating an absence of macrophase separation. On the other hand, Figure 9(b) shows discontinuous cavities that were not observed in any of the transparent films. Figure 9(c) shows micron-sized pores typical of systems exhibiting phase separation characteristics. Note that the micrograph in Figure 9(c) is at 10 times higher magnification than Figure 9(b). However, examination of film in Figure 9(b) at very high magnifications did not show any porosity associated with this specimen. The pores or cavities act as defect sites in strain–stress testing, which lead to significantly lower moduli for films 5 and 9.

Morphological Analysis

Small angle x-ray scattering (SAXS) was also used to discern changes in the morphologies of the cast films. SAXS studies on CA and CAG films with varying initial concentration of TEOS were carried out. (These OIH films were prepared with a different CAG than those described in Table I. The level of grafting was approximately one grafted substituent per six CA repeat unit. However, they were prepared under the same conditions as the OIH films described in Table I.) Figure 10 shows the scattering intensity as a function of the inverse of scattering length for CA (□) and CAG with 0 (▽), 19 (●), 31 (△), and 38% (○) initial TEOS. All of these films were transparent, indicating the absence of macrophase separation. The films cast from CAG were also crosslinked. The scattering behavior of CA (□) and CAG (▽) with 0% initial TEOS are very similar, indicating that the presence of grafted triethoxysilane groups does not lead to phase separation. Upon addition of 19% of TEOS (●), an increase in the scattering intensity in the range of 0.15 to 4 nm^{-1} is observed. A systematic increase in the scattering intensity also is observed with further increases in

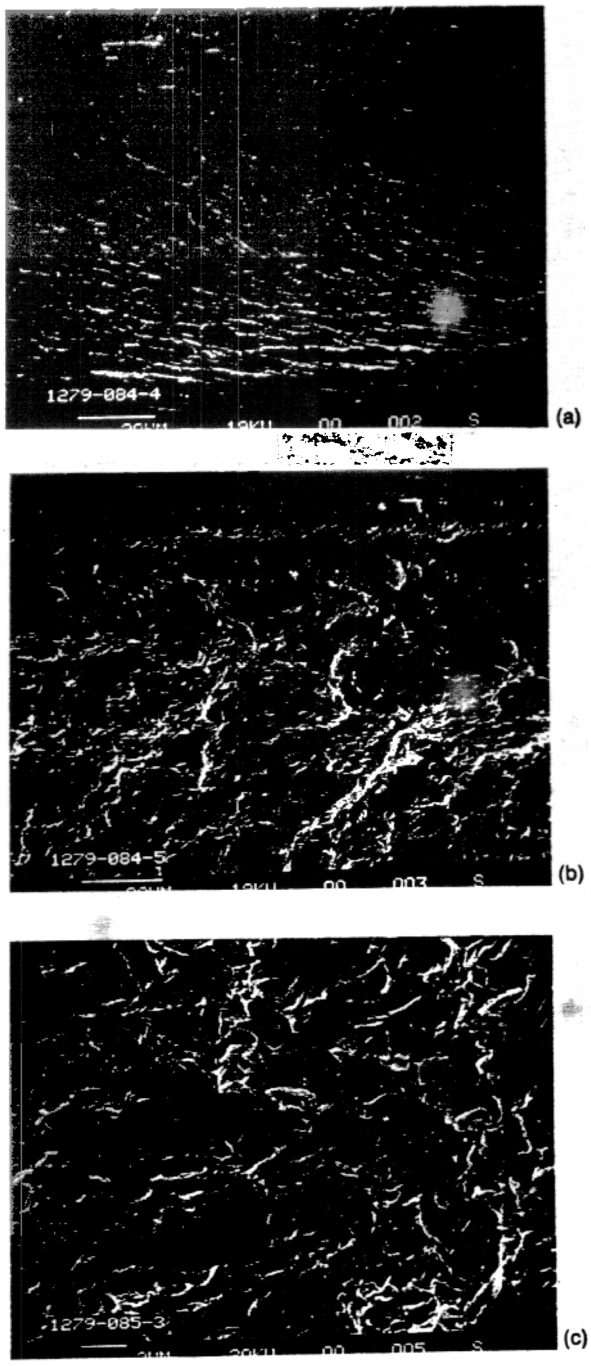

Figure 9 Scanning electron micrograph of OIH films (a) 3, (b) 5, and (c) 9 of Table I.

the initial level of TEOS. The SAXS data indicate that the addition of TEOS results in the formation of a second homogeneously dispersed inorganic phase within the polymer matrix. These results indicate that increasing the initial TEOS content results in an increase in the size of this second phase. It may be reasonable to assume that the films dis-

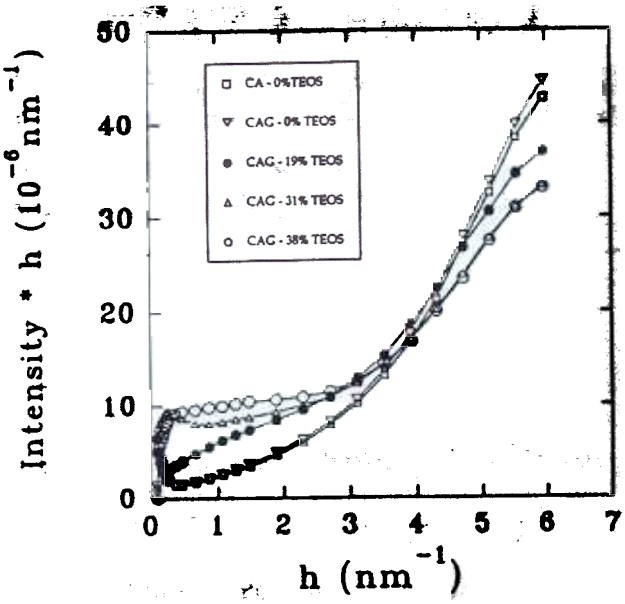

Figure 10 Small-angle x-ray scattering of OIH films showing the effect of initial TEOS concentration on the size of scattering sites.

cussed in Table I would also exhibit similar concentration-dependent, microscopic phase-separation phenomenon.

DISCUSSION

Formation of these CA OIH films involves a series of very complex and interrelated chemical and physical processes that control the properties of the final OIH film. In this discussion, we will try to highlight these chemical and physical processes, their interactions, and their effect on the properties of the resultant films. There are three major processes that can influence the final properties of the CA OIH films: preparation and number of the grafted triethoxysilane groups, chemical reactions and physical processes that occur during the sol–gel process, and physical processes associated with the loss of casting solution solvent.

The first of these processes involves the production of the CAG starting material through a series of chemical reactions. The level of grafting can be controlled reasonably well through careful manipulation of the stochiometry of the two reactive components, 3-isocyanatopropyl triethoxysilane and cellulose acetate hydroxyls. However, during the isolation and drying step crosslinking reactions of the triethoxysilane groups may take place. The grafted triethoxysilane groups are sensitive to small amounts of water, which can be chemisorbed on the polymer or present in the "dry" solvent. The CAG can undergo crosslinking during the initial grafting reactions or in the solid state in the absence of any catalyst. These premature reactions were minimized by keeping the starting material under a blanket of nitrogen as well as minimizing the time between the chemical grafting and dense film casting steps. However, insoluble gel particles were removed from the CAG solution that was used in preparation of OIH films.

The second process involves the chemical reactions that control the hydrolysis and condensation reactions of the triethoxysilane groups attached to the CA and the tetraethoxysilane groups of the TEOS. The rates of these sequential chemical reactions can be controlled in a fairly direct manner by controlling the amount of HCl catalyst and water that are added to the reaction mixture. However, there are second-order effects that are much less easily controlled and poorly understood. For example, very little is known about the direct condensation reactions between CA hydroxyls and silanol groups. Our recent work with ungrafted CA and TEOS has demonstrated that crosslinked insoluble films can be formed with these two components. Presumably these same direct condensation reactions are occurring in the CAG/TEOS system. These direct condensation reactions can contribute to the formation of a greater number of crosslinking sites than would be anticipated from the simple grafting chemistry.

An additional second-order effect is the difference in the relative mobility of silanol groups on TEOS molecules and silanol groups grafted into the CA backbone. Even though the chemical reactivity of these silanol groups may be very similar, the relative mobility of the two types of groups in the viscous casting solution as it approaches the gel point can have an impact on the number of crosslinking sites and the molecular weight between crosslinking sites. For example, as a CAG solution with no added TEOS approaches the gel point the lack of molecular mobility of the polymer backbone could limit the opportunities for the grafted silanol groups to crosslink. However, in the case of a CAG solution with 30% TEOS approaching the gel point, the higher mobility of the silanols on TEOS could allow for additional condensation reactions between the relatively immobile grafted silanols and highly mobile "free" silanols. These condensation reactions could extend the length and functionality around the grafted site and increase the probability of forming

an effective crosslinked junction. Addition of more TEOS should also increase the potential for direct condensation reactions between hydroxyls on the CA and the TEOS silanol groups.

The third and final effect is related to the rate of evaporation of solvent (acetone) from the cast films, which influences the mobility and solubility of the CAG, and, thus, dictates the sol–gel reaction rates and the potential for solvent/nonsolvent phase separation.[11] The viscosity of the solutions used for preparation of the OIH films is governed primarily by the molecular weight and concentration of the CAG. As the casting solvent evaporates, the viscosity of the casting solution increases and the mobility of the CAG decreases. The impact of the mobility of the reactive groups was discussed above.

In addition to affecting the mobility of the polymer chains, evaporation of the acetone solvent can also affect the thermodynamic state of the CAG solution resulting in macroscopic phase separation. Two of the films (5 and 9) were macrophase separated. This type of macrophase separation is common for CA films and is the basis of the original discovery of CA asymmetric membranes. These original CA asymmetric membranes were cast from a ternary mixture of a polymer (CA), a good solvent (acetone), and a nonsolvent (water).[12] As the acetone solvent evaporates, the relative concentration of both the CA and the nonsolvent, TEOS in the case of these OIH films, increases. This relative increase in the concentration of the nonsolvent for CA will act as the driving force for solvent/nonsolvent macrophase separation. Macrophase separation causes the polymer solution to form polymer-rich (TEOS-lean) and polymer-lean (TEOS-rich) phases. With complete evaporation of the acetone the TEOS-rich domains become large voids, rich in TEOS. As one can imagine, the formation of these domains will affect the concentration of TEOS in the CA component and potentially allow for the disposition of TEOS on the walls of the cavities that are formed during the macrophase separation process. This complex set of variables is not well understood for this system, but obviously can affect the properties of the final CA OIH film.

CONCLUSIONS

The solvent resistance properties of the crosslinked OIH films are far superior to those of uncrosslinked, as evident by the insolubility of the crosslinked films in acetone from which they were initially cast. The mechanical properties slightly improved over the unmodified cellulose acetate film. Lack of significant improvement in the mechanical properties, e.g., modulus or ultimate strength, may be attributed to the fact that the starting polymer (CA) is a high modulus glassy polymer. The mechanical properties of the OIH films in the rubbery state, as evidenced by the DMA results, are far superior to the mechanical properties of the starting CA.

The use of sol–gel chemistry to form OIH films is complicated by a number of competing chemical and physical processes. Some observed scatter in the data presented in this study may be attributed to the inability to control the reaction rates. This study suggests that grafting of 3-isocyanatopropyl triethoxysilane on the cellulose acetate backbone can successfully be achieved. It was also found that slow crosslinking of the grafted polymer in the solid state can occur in the absence of any catalyst. The solid-state NMR showed that the sol–gel reactions do not proceed to completion. This is probably because of film-casting technique where solvent evaporation can hasten the gelation/solidification process and, hence, significantly alter reaction rates. The TGA and SAXS analyses indicate the presence of a second homogeneously dispersed phase within the polymer matrix on both a macroscpoic and microscopic scale. At the present time, it is not clear what parameters control the observed solvent/nonsolvent phase separation phenomenon with the films cast from CAG^+. One only can speculate that presence of water and TEOS certainly can cause phase separation because both of these components are considered as nonsolvents for a cellulose acetate/acetone system. The phase separation phenomenon is currently under further investigation.

The authors would like to thank Dr. Yan Chen and Professor Don L. Williamson of the Colorado School of Mines for their help in obtaining and interpreting the small angle x-ray scattering data. We would also like to thank Dr. Mark Davis of the National Renewable Energy Laboratory for his assistance in obtaining and interpreting the solid-state NMR data. The financial support of Department of Energy Advanced Industrial Concepts Program is greatly appreciated.

REFERENCES

1. R. C. Mehrotra, in *Structure and Bonding*, R. Reisfeld and C. K. Jorgensen, Eds., **77**, 1 (1992).

2. J. D. Mackenzie and D. R. Ulrich, in *Sol-Gel Optics, Proceedings of SPIE-The International Society for Optical Engineering*, D. R. Ulrich and J. D. Mackenzie, Eds., **1328**, 1 (1990).
3. L. C. Klein and J. G. Garvey, in *Better Ceramics Through Chemistry*, C. J. Brinker, D. E. Clark, and D. R. Ulrich, Eds., **32**, 33 (1984),
4. H. Schmidt, H. Scholze, and A. Kaiser, *J. Non-Crystalline Solids*, **63**, 1 (1984).
5. H. Dislich, *J. Non-Crystalline Solids*, **57**, 371 (1983).
6. H. H. Huang, B. Orler, and G. L. Wilkes, *Macromolecules*, **20**, 1322 (1987).
7. G. Philipp and H. Schmidt, *J. Non-crystalline Solids*, **63**, 283 (1984).
8. J. L. Noell, G. L. Wilkes, and D. K. Mohanty, *J. Appl. Polym. Sci.*, **40**, 1177 (1990).
9. H. H. Huang, G. L. Wilkes, and J. G. Carlson, *Polymer*, **30**, 2001 (1989).
10. R. H. Glaser, G. L. Wilkes, and C. E. Bronniman, *J. Non-Crystalline Solids*, **113**, 73 (1989).
11. S. S. Shojaie, W. B. Krantz, and A. R. Greenberg, *J. Membrane Sci.*, **94**, 281 (1994).
12. Kesting, R. E., *Synthetic Polymeric Membranes: A Structural Perspective*, 2nd Ed., John Wiley & Sons, New York, 1985.

Received January 12, 1995
Accepted March 7, 1995